Extending the Tracking Range for Prospective Motion Correction using a Single In-bore Camera and the Self-encoded Marker

Christoph Forman[1,2], Murat Aksoy[1], Matus Straka[1], Joachim Hornegger[2], Roland Bammer[1]
[1]Department of Radiology, Stanford University, Stanford, CA, United States [2]Pattern Recognition Lab, Department of Computer Science, Friedrich-Alexander-University Erlangen-Nuremberg, Erlangen, Germany

INTRODUCTION – Patient motion during data acquisition is still a challenging problem for brain MRI. Motion can lead to considerable image artifacts, which often lowers diagnostic confidence or produce non-diagnostic images. Recently, methods were proposed to correct for motion by tracking the patient pose with a camera system during the scan and try to adapt for possible changes in real-time [1,2,3]. Aksoy *et al.* [3] introduced an approach using a single in-bore camera mounted on an 8-channel head coil to track the patient during an MRI exam. A checkerboard marker is attached to the patient's forehead to determine and follow the patient's pose in real time. A drawback of this approach is the restricted field of view (FOV) of the in-bore camera, which originates from a close camera-marker distance (5cm – 7cm). For reliable pose estimates, the checkerboard marker has to be entirely inside the FOV of the tracking camera to establish the point correspondences between the detected feature points and the object coordinates. This in turn lowers the possible tracking range. To overcome this limitation, we developed a self-encoded marker based on the checkerboard pattern.

MATERIALS and METHODS – (a) System Description: Each feature point on this marker is encoded by a unique and rotationally invariant 9-bit code, which is embedded on a 3x3 grid within the black squares of the pattern. For the pose estimation, first, the black squares of the marker are detected on the camera image. Then, each position encoding in the interior of these quads is recognized by binary classification. Finally, the position of the marker – relative to the camera – is estimated using the corners of the detected quads and their corresponding 3-D object coordinates. Thereby, the pose of the marker is estimated although parts of the marker are occluded by objects within the camera image or are outside the camera FOV (see Figure 1). That way, the marker detection is independent of the camera FOV and the tracking range is increased by the size of the marker. For the motion correction, the detected motion of the marker relative to an initial frame of reference is transformed into the scanner coordinate system as described in [2]. **(b) In-vivo Experiments:** In order to compare the pose tracking of the self-encoded and the conventional checkerboard marker, an *in-vivo* experiment was performed using an axial 3D SPGR sequence with TR/TE 9.5ms/4.1ms, flip angle=20°, slice thickness=1.5mm, FOV=24cm, and a resolution of 192x192x96. During the scan, the volunteer was asked to move his head every 30 seconds. Pose data from either the new self-encoded marker or the checkerboard marker were used to adapt the scanner geometry to compensate for this motion. For reference, an additional scan was conducted where the patient was asked to maintain still.

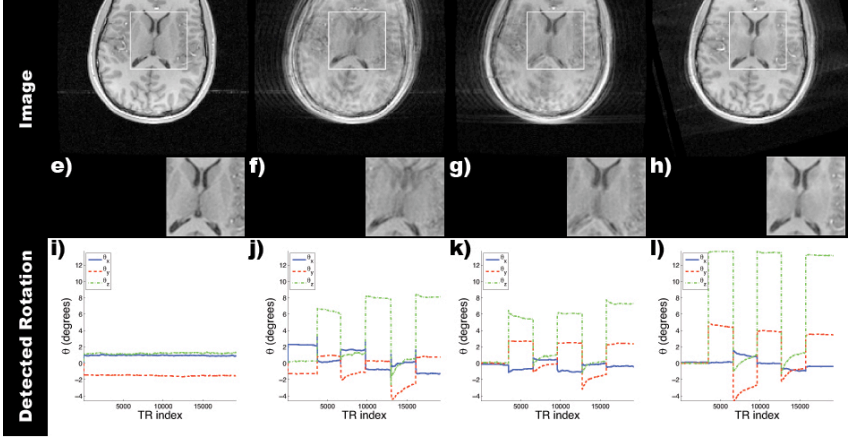

Figure 2 – Results of the *in-vivo* experiment using an axial 3D SPGR scan: **(a)** Reference scan without motion; **(b)** Scan with motion and no correction; **(c)** Scan with motion and prospective correction using the checkerboard marker; **(d)** Scan with motion and prospective correction using the self-encoded marker; **(e-h)** Magnification of window in (a-d); Corresponding motion plots using the checkerboard **(i-k)** and self-encoded marker **(l)**.

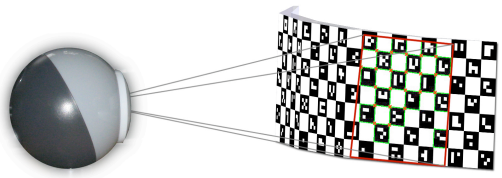

Figure 0 – The self-encoded marker is detected in the camera FOV although only a portion of it is visible to the camera field of view (red square). Common corners of all correctly detected quads (green squares) are used for the pose estimation.

RESULTS – Figure 2a-d show the resulting images for the *in-vivo* experiment. A magnification of the window in these images is shown in Figure 2e-h. The limitation of the checkerboard marker restricted the possible head rotation of the volunteer to a range of 8° (Figure 2j,k). Using the self-encoded marker the motion correction system was able to cover an extended tracking range. However, for a fair comparison of the image quality of the motion-corrected images, we asked the volunteer to limit the head rotation to 13° (Figure 2l). As seen in Figure 2b,f the anatomical structure shows significant artifacts because of uncorrected motion during data acquisition. Using the pose updates of the checkerboard marker, these artifacts were reduced (Figure 2c,g). Due to the fact that this marker was parallel to the camera image plane, these updates were not accurate enough to fully compensate the motion as seen in Figure 2g. Despite an extended range of the performed motion using the self-encoded marker, the system was able to successfully remove the majority of motion-induced errors (Figure 2d,h). The correlation between the reference and the motion-corrupted image resulted in a coefficient of 0.9077. While the pose updates of the checkerboard marker increased this correlation to 0.9361, the self-encoded marker achieved a correlation of 0.9707. A statistical comparison [4] of the resulting correlation showed a significant improvement of the self-encoded marker relative to the checkerboard marker in terms of image quality ($p < 0.001$, $|u| = 216.53$).

DISCUSSION – In this study, we presented a new marker design, which is not restricted by the camera FOV. This way, by recognizing a portion of the marker visible in the camera FOV, this approach provides an extended tracking range. Furthermore, the *in-vivo* experiments using the self-encoded marker showed an improvement in terms of image quality compared to the checkerboard marker.

REFERENCES – [1] Zaitsev *et al.*, NeuroImage, 31:1038-1050, 2006. [2] Aksoy *et al.*, ISMRM, 2008 [3] Aksoy *et al.*, ISMRM, 2009 [4] *Maier A.*, Speech of Children with Cleft Lip and Palate: Automatic Assessment, p. 49, Logos, Berlin, Germany, 2009.

ACKNOWLEDGEMENTS – This work was supported in part by the NIH (1R01EB008706, 5R01EB002711, 1R01EB006526, 1R21EB006860, P41RR09784), Lucas Foundation, Oak Foundation, Bavarian California Technology Center, and GE Healthcare.